World Academy of Science, Engineering and Technology
International Journal of Materials and Textile Engineering
Vol:9, No:10, 2015

Continuous Fixed Bed Reactor Application for Decolourization of Textile Effluent by Adsorption on NaOH Treated Eggshell

M. Chafi, S. Akazdam, C. Asrir, L. Sebbahi, B. Gourich, N. Barka, M. Essahli

***Abstract*—**Fixed bed adsorption has become a frequently used industrial application in wastewater treatment processes. Various low cost adsorbents have been studied for their applicability in treatment of different types of effluents. In this work, the intention of the study was to explore the efficacy and feasibility for azo dye, Acid Orange 7 (AO7) adsorption onto fixed bed column of NaOH Treated eggshell (TES). The effect of various parameters like flow rate, initial dye concentration, and bed height were exploited in this study. The studies confirmed that the breakthrough curves were dependent on flow rate, initial dye concentration solution of AO7 and bed depth. The Thomas, Yoon–Nelson, and Adams and Bohart models were analysed to evaluate the column adsorption performance. The adsorption capacity, rate constant and correlation coefficient associated to each model for column adsorption was calculated and mentioned. The column experimental data were fitted well with Thomas model with coefficients of correlation $R^2 \geq 0.93$ at different conditions but the Yoon–Nelson, BDST and Bohart–Adams model (R^2=0.911), predicted poor performance of fixed-bed column. The (TES) was shown to be suitable adsorbent for adsorption of AO7 using fixed-bed adsorption column.

***Keywords*—**Adsorption models, acid orange 7, bed depth, breakthrough, dye adsorption, fixed-bed column, treated eggshell.

I. Introduction

IN industry, the wastewater is generated in large volumes. Water contamination resulting from dyeing and finishing in textile industry is of a major concern. Discharging large amount of dyes in water resources accompanied with organics, bleaches, and salts can affect the physicochemical properties of freshwater. The worldwide high level of dye production and their extensive use in many applications generate coloured wastewaters which cause severe water pollution. A large number of reactive dyes are azo compounds that are linked by an azo. In addition to their unwanted colors, some of these dyes effluents are generally considered to be highly carcinogens and toxic. In addition, the removal of dyes from effluents is important since reactive dyes are highly soluble in water. So the most commonly used conventional methods for the removal of heavy metals from wastewater like physicochemical and biological treatment, coagulation, membrane process, ion exchange, chemical precipitation, solvent extraction and photocatalysis etc... are available for the treatment of coloured industrial wastewaters. However, these methods suffer from so many drawbacks due to the difficulty of removal from the effluent [1].

Adsorption is known to be a promising technique, which produces good quality effluents with low levels of dissolved organic compounds such as dyes. It has been recognized as an effective process in most of the industrial water and wastewater treatment. Adsorption process has long been used in the removal of heavy metals and other hazardous materials such as, color, odor, and organic pollution. Although activated carbons have been most widely used as adsorbents in wastewater treatment processes [2], [3], there is growing interest in using low cost, commercially available materials for the adsorption of dyes.

The number of research currently being done on the use of low cost adsorbent for metal removal from aqueous solution produced from renewable and cheaper precursors which are mainly industrial and agricultural by-products attests of the evident recent attention focusing on this field. A wide variety of materials such as coir pith [4], orange peels [5], palm-shell [6], rice straw [7], cellulose beads [8] sunflower [9] peat [10], palm-fruit [11], silica fumes [12], natural zeolite [13], montmorillonite, and kaolinite [14] has been investigated and used for the removal of dyes from industrial effluents because they are cheaper than commercial activated carbons and their sheetlike structures also provide high specific surface area. The interactions between low-cost adsorbents and dyes (adsorbates) are extensively studied through batch equilibrium) and column studies.

In the past, the adsorption of dyes from aqueous solutions onto Eggshell mostly focused on the equilibrium and contact-time kinetic studies, isotherm, and thermodynamic studies in batch modes of MB removal onto TES at different parameters (temperature, pH, initial concentration, and adsorbent dose). Batch adsorption processes may not be a convenient method for the industrial scale to deal with high flow rates. Batch experiments are usually done to measure the effectiveness of

S. Akazdam, C. Asrir, PhD students, are with the Laboratory of Environment, Processes and Energy (LEPE). High School of Technology, University Hassan II Casablanca Morocco (e-mail: said.akazdam@gmail.com; asrir1chaimaa@gmail.com).

M. Chafi, L. Sebbahi, B. Gourich, professors, are with the University Hassan II, High School of Technology, Laboratory of Environment, Processes and Energy (LEPE). Casablanca Morocco (phone:0616844829; fax: 212522252245; e-mail: chafimoham@gmail.com, l.sebbahi@yahoo.fr; gourichgp@hotmail.com).

N. Barka is with the Univ Hassan 1, Laboratoire des Sciences des Matériaux, des Milieux et de la Modélisation (LS3M), BP.145, 25000 Khouribga, Morocco (e-mail: barkanoureddine@yahoo.fr).

M. Essahli is with the Univ Hassan 1, Laboratory of Applied Chemistry and Environment, Faculty of Science and Technology, BP 577, Settat, Morocco (e-mail: essahli_mohamed@yahoo.fr).

adsorption for removing specific adsorbates as well as to determine the maximum adsorption capacity.

The continuous adsorption in fixed-bed column is often desired from industrial point of view. It is simple to operate and can be scaled-up from a laboratory process [15]. A continuous packed bed adsorber does not run under equilibrium conditions and the effect of flow condition (hydrodynamics) at any cross-section in the column affects the flow behaviour downstream. Breakthrough determines bed height and the operating life span of the bed and regeneration times [16]. Adsorption in fixed-bed columns using activated carbon has been widely used in industrial processes for the removal of contaminants from aqueous textile industry effluents, since it does not require the addition of chemical compounds in the separation process [17].

Adsorption in a fixed bed column can be used continuously under high effluent flow rates and it has been used in many pollution control processes such as removal of ions by an ion-exchange bed or removal of toxic organic compounds by carbon adsorption [18]. In this study, the activated carbon prepared from Eggshell has been tested for removal of aqueous solutions. In this paper, Eggshell is used to remove azo dye (AO7) from aqueous solution through column studies.

The objective of this study was to investigate the adsorption potential of AO7 onto TES fixed-bed. The important design parameters such as inlet concentration of dye solution, fluid flow rate and column bed height [19] were investigated using a laboratory scale fixed-bed column. The breakthrough curves for the adsorption of AO7 were analyzed using Adam's–Bohart, Thomas and Yoon–Nelson models at different flow rates, bed heights, and initial concentrations. Further, modeling on the adsorption dynamics of the fixed bed was presented and finally the correlation between the model and the experimental data was compared.

II. Material and Methods

A. Adsorbate

AO7 used in this study was purchased from Sigma–Aldrich (M). (AO7) has molecular formula $C_{16}H_{11}N_2NaO_4S$ (Mol. wt. 350.33 g/mol). The maximum wavelength of this dye is 485 nm. The dye stock solution was prepared by accurately dissolving a weight of dye in distilled water to the concentration of 1 g/L. The experimental solutions were obtained by diluting the dye stock solution in accurate proportions to needed inlet concentrations. The chemical structure of (AO7) is shown in Fig. 1.

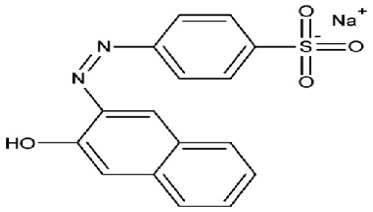

Fig. 1 Chemical structure of the acid orange 7

B. Preparation and Characterization of Eggshell Powder

Adsorbents, in the form of eggshell, were collected from house and local restaurants. To remove impurity and pollutants and to prevent decomposition, eggshells were first washed several times in tap water, and then boiled in distilled water to remove any adhering dirt. The washed materials were then dried at 100°C for 24 h in the dry oven. The dried eggshell was ground using ball mill. The powdered materials were sieved into a size range of 0.711 to 0.250 mm. Finally, the sieved material was treated with sodium hydroxide 2N NaOH for 2 h then the sample was neutralized and dried in the oven at 100°C for 24 h. Before each use, we put the resulting adsorbent, TES in a dryer to remove moisture. The chemical composition of eggshell is composed of: 94 to 97% calcium carbonate; 3% to 6% protein; 1% of various minerals (including magnesium, potassium and trace amounts of iron, sulfur and phosphorus). Fourier Transform Infrared (FTIR) analysis was applied to determine the surface functional groups, using FTIR spectrophotometer (SCO TECH SP-FTIR-1). The spectra were recorded from 4000 to 400 cm^{-1}[20].

C. Sorption Capacity and Removal Efficiency

Sorption capacity (q) of AO7 was defined as:

$$q_e = (C_0 - C_e)x\frac{v}{m} \quad (1a)$$

where; q_e is the uptake capacity (mg/g), C_0 and C_e (mg/L) are the liquid-phase concentrations of AO7 at initial and any time t, respectively, v is the volume of the solution (ml) and m is the mass of the adsorbent (g). Biphasic samples filtration was carried out using disposable syringe filters with 0.45 µm pore size and showed first no interaction with the dye during the sampling. The analysis of the instantaneous concentration C_t in the filtered liquid phase was performed using a double beam UV-visible absorption SPECORD 250+ spectrophotometer using the AO7 maximum absorbance wavelength (λmax = 485 nm). The linearity of Beer-Lambert law was checked for concentration ranging from 1 to 50 mg/L with a correlation coefficient $R^2 = 0.9997$.

In addition, the removal efficiency (Re) is calculated according to:

$$Re(\%) = 100x(C_0 - C_e)/C_0 \quad (1b)$$

where C_0 is the initial concentration of dye in solution (mg/L), and C_e is the final dye concentration in aqueous solution after phase separation (mg/L).

III. Sorption Experiments in Fixed-Bed Technique

A. Experimental Procedures

The fixed bed experiments were carried out in a glass column of 2 cm internal diameter, 30 cm of the length height and three sampling points at 5 cm intervals. A known quantity of the prepared activated carbon TES was packed in the column to yield the desired bed height of the adsorbent 50,

100 and 150 mm (equivalent to 3.5, 7 and 10,5 g of activated carbon) with a layer of glass wool at the bottom. Distilled water was passed through the column in order to remove impurities from the adsorbent. Three flow rates (2, 4 and 6 mL/min) were pumped to the top of the packed column by using peristaltic pump (name) with different initial dye concentrations (5, 30, 50, 80 mg/L). The samples of AO7 solutions at the outlet of the column were taken at regular time intervals and the concentration of dye was measured using an UV–visible spectrophotometer (Neptune Chemical Pump) at wavelength of 485 nm. Fixed bed studies were terminated when the column reached exhaustion. The experiments were carried out at temperature of 301 K (28 ±1 ◦C) without any pH adjustment.

The schematic diagram of fixed bed column used in adsorption study is shown in Fig. 2. The experimental detail is given in Table I. Briefly, the experiment was carried out by passing through column (packed with 21 g of TES) with controlled flow rate and pH. The pH of influent was maintained by 1.0 N HCl or 1.0 N NaOH during experiments.

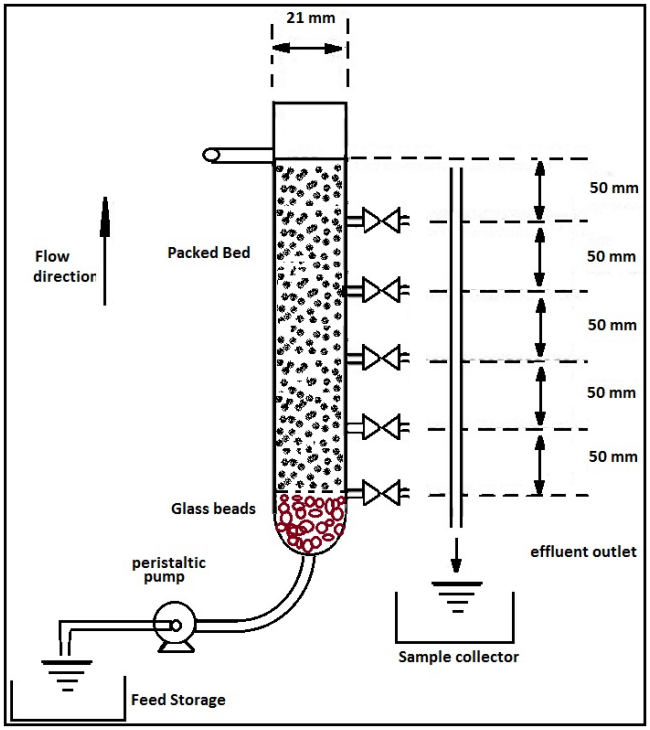

Fig. 2 Schematic diagram of fixed bed column used in adsorption study of AO7 onto TES

TABLE I
EXPERIMENTAL DETAILS FOR COLUMN ADSORPTION OF AO7 ONTO TES

EFFECT OF SYSTEM	Flow rate (mL/min)	[AO7] (ppm)	Bed height (cm)
Flow rate	2, 4 and 6	30	15
Initial Concentration	15	5, 30, 50 and 80	15
Bed height	15	200	5, 10 and 15

B. Analysis of Fixed-Bed Column Data

For good design of fixed bed system, it is important to predict the breakthrough curve for effluent parameters. The time for breakthrough appearance and the shape of the breakthrough curve are very important characteristics for determining the operation and the dynamic response of an adsorption fixed-bed column. The breakthrough curves show the loading behavior of dye to be removed from solution in a fixed-bed column. It is usually expressed in terms of adsorbed dye concentration (C_{ad}), inlet AO7 concentration (C_0), outlet AO7 concentration (C_t) or normalized concentration defined as the ratio of outlet AO7 concentration to inlet AO7 concentration (C_t/C_0) as a function of time for a given bed height [21].

C. Column Adsorption Model

To design a column adsorption process, it is necessary to predict the breakthrough curve or concentration-like profile and adsorption capacity of the adsorbent for the selected adsorbate under the given set of operating conditions. It is also important for determining maximum sorption column capacity, a significant parameter for any sorption system. A number of mathematical models have been developed for the evaluation of efficiency and applicability of the column models for large-scale operations. The Thomas, Yoon–Nelson, and Adams and Bohart Models were used to predict the dynamic behavior of adsorbent adsorbate system in this study.

1. The Thomas Model

The Thomas solution is one of the most widely used models in column performance studies. Thomas model [22] assumes plug flow behavior in the bed. This model is suitable for adsorption processes where the external and internal diffusion limitations are absent. The expression by Thomas for an adsorption column [23] is given as:

$$q_e = \frac{RT}{b_t} \ln(k_t C_e) \tag{2}$$

Thomas model is given in linear form by:

$$Ln\left[\frac{C_0}{C_t} - 1\right] = \left[(k_{Th} q_0 x / Q) - k_{Th} C_0 t\right] \tag{3}$$

where; k_{TH} (mL/min mg) is the Thomas rate constant; q_0 (mg/g) is the equilibrium AO7 uptake per g of the adsorbent; maximum sorption capacity (q_e); C_0 (mg/L) is the inlet dye concentration; C_t (mg/L) is the outlet effluent dye concentration at time t; x (g) the mass of the used adsorbent, Q (mL/min) the flow rate and t (min) stands for flow time. The value of C_t/C_0 is the ratio of outlet to inlet AO7 concentrations.

The parameters of Thomas model (k_{Th} and q_e) can be determined from a plot of $Ln\ [(C_0/C_t) - 1]$ against time (t) at a given flow rate.

2. The Adams and Bohart Model

Adam's–Bohart model [24] established the fundamental equations describing the relationship between C_0/C_t and t in a continuous system. The Adam's–Bohart model is used for the description of the initial part of the breakthrough curve. The

model proposed assumes that the adsorption rate is proportional to both the residual capacity of the TES and the concentration of the sorbing species. The expression of Adams–Bohart is:

$$t = (N_0 x / C_0 v) - \left[\left(Ln\left(\frac{C_0}{C_t} - 1\right)/(C_0 k_{AB})\right)\right] \quad (4)$$

The linear form of Adam-Bohart model is given by:

$$Ln\left(\frac{C_t}{C_0}\right) = k_{AB} C_0 t - k_{AB} N_0 Z / F \quad (5)$$

where; C_0 and C_t (mg/L) are the inlet and effluent dyes concentration, k_{AB} (L/mg min) is Bohart–Adams rate constant, F (cm/min) is the linear velocity calculated by dividing the flow rate by the column section area, Z (cm)is the bed depth of column, and N_0 (mg/L) is the adsorption capacity of the adsorbent are dependent on flow rate, initial ion concentration and bed height which are calculated from plot of $Ln(C_t/C_0)$ versus time, t.

The parameters k_{AB} and N_0 were determined from the intercept and slope of linear plot of $Ln(C_t/C_0)$ against time (t), respectively.

3. The Yoon–Nelson Model

Yoon and Nelson [25] developed a model based on the assumption that the rate of decrease in the probability of adsorption of adsorbate molecule is proportional to the probability of the adsorbate adsorption and the adsorbate breakthrough on the adsorbent. The Yoon–Nelson linearized model for a single component system is expressed as:

$$Ln\left(\frac{C_t}{C_0 - C_t}\right) = k_{YN} t - \tau k_{YN} \quad (6)$$

where; k_{YN} (1/min) is the Yoon–Nelson rate constant, τ (min) is the time in required for 50% adsorbate breakthrough, and t is the sampling time. A plot of $Ln(C_t/(C_0 - C_t))$ versus t gives straight line curve with a slope of k_{YN} and intercept of $-\tau k_{YN}$. Based upon the obtained value of τ, the adsorption capacity, q_{0YN}, was found out using:

$$q_{0YN} = q(total)/X = C_0 Q \tau / (1000X) \quad (7)$$

So, adsorption capacity (q_{0YN}) related to Yoon–Nelson varies as an inlet dye concentration (C_0), flow rate (Q), 50% breakthrough time derived from Yoon–Nelson equation (τ) and weight of adsorbent (X).

4. Wolborska Model

Wolborska [26] based his model on general mass transfer rate of diffusion mechanism. It applies for low concentrations for breakthrough curves. The simplified form of the equation is given as:

$$\partial q/\partial t = V_m dq/dH = B_a(C_b - C_i) \quad (8)$$

where; C_b the solute concentration in the bulk liquid (mg/l), C_i the liquid migration rate through the bed (cm/min), H the bed depth (cm), and Ba the kinetic coefficient of the external mass transfer (min^{-1}).

The solution of the differential equation is:

$$ln\left(\frac{C}{C_0}\right) = \frac{B_a C_0}{q_1} t - \frac{H.B_a}{\upsilon_m} \quad (9)$$

IV. Results and Discussion

A. Characterization of the Adsorbent

The characterization of the adsorbent, TES was done in the previous papers where the TES was used for removal of MB through batch kinetics experiments, isotherm, and thermodynamic studies.

B. Effect of Initial Dye Concentration

The variable effect of inlet AO7 concentration from 5 to 80 mg/L on the adsorption of AO7 in the TES containing column was studied at 10 cm constant adsorbent bed height, 4 mL/min solution flow rate, 7.04 constant AO7 solution pH and 301 K temperature. The breakthrough curve, thus deduced is shown in Fig. 2.

The breakthrough curves for all initial concentrations were drawn between the time and C_t/C_0 as shown in Fig. 3. It is observed that the break point time decreased with increased initial AO7 concentration from 5 to 80 mg/L. On increasing the initial ion concentration, the breakthrough curves became steeper and breakthrough volume decreased because of the lower mass-transfer system from the bulk solution to the adsorbent surface.

It is illustrated that the breakthrough time slightly decreased with increasing inlet AO7 concentration. At lower inlet AO7 concentrations, breakthrough curves were dispersed and breakthrough occurred slower. As influent concentration increased, sharper breakthrough curves were obtained. This can be explained by the fact that a lower concentration gradient caused a slower transport due to a decrease in the diffusion coefficient or mass transfer coefficient. The larger the inlet concentration, the steeper is the slope of breakthrough curve and smaller is the breakthrough time. These results demonstrate that the change of concentration gradient affects the saturation rate and breakthrough time, or in other words, the diffusion process is concentration dependent. The adsorption capacity was expected to increase with increasing the inlet concentration because a high concentration difference provides a high driving force for the adsorption process.

The breakdown time and exhaust time were increasing with decreasing initial dye concentration. The breakthrough and the exhausting times for different dye concentrations of 5, 30, 50 and 80 ppm were deceased as 48, 38, 30, and 15 min and 160, 140, 130, and 80 min, respectively. This is due to the TES getting saturated more quickly at higher initial reactive dye concentrations. Thus, breakthrough and the exhausting times for the higher influent concentration were less or earlier than those for the lower influent concentration

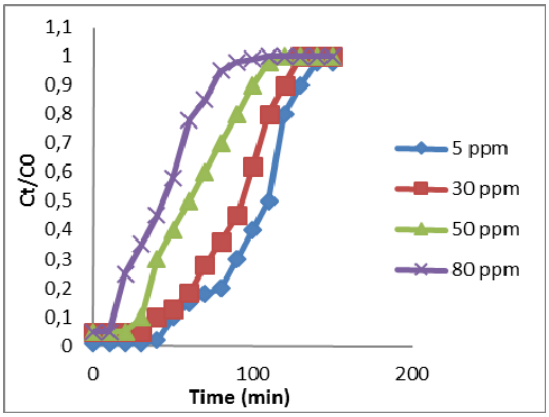

Fig. 3 Breakthrough curves for AO7 adsorption column by TES at different initial AO7 concentrations

C. Effect of the Solution Flow Rate

The effect of the flow rate on the adsorption of AO7 using the TES was investigated by varying the flow rate (2, 4 and 6 mL/min) using 30 mg/L initial AO7 concentration, 10 cm bed height, pH 7.04 at 301 K., as shown by the breakthrough curve in Fig. 4.

Fig. 4 shows that the breakthrough curve occurred faster at higher flow rate. This is because the lower residence time of the influent in the column, thus reducing the contact time between AO7 and the TES.

It was shown that breakthrough generally occurred faster with higher flow rate. Breakthrough time reaching saturation was increased significantly with a decreased in the flow rate. When at a low rate of inlet AO7 had more time to contact with TES that resulted in higher removal of AO7 ions in column. The variation in the slope of the breakthrough curve and adsorption capacity may be explained on the basis of mass transfer fundamentals. The reason is that at higher flow rate the rate of mass transfer gets increased, i.e. the amount of dye adsorbed onto unit bed height (mass transfer zone) gets increased with increasing flow rate leading to faster saturation at higher flow rate. At a higher flow rate, the adsorption capacity was lower due to insufficient residence time of the solute in the column and diffusion of the solute into the pores of the adsorbent, and therefore, the solute left the column before equilibrium occurred.

The column adsorption experiment was carried out at different flow rates of 2, 4and 6 mL/min using initial AO7 concentration of 30 ppm and bed height of 10 cm at neutral pH. The resulting breakthrough graph is mentioned in Fig. 4, in which breakthrough occurred faster with higher flow rate of 6 mL/min. And breakthrough curve of the lower flowrate of 2 mL/min tended to be more gradual, meaning that the column was difficult to be completely exhausted. Increasing the flow rate in the TES bed caused a decrease in AO7 removal efficiency. This is attributed to the fact that low contact time between the adsorbate and adsorbent reduces the adsorption efficiency in the TES bed. In addition, at higher flowrates, the movement of adsorption zone along the bed is faster reducing the time for adsorption of dye on the TES bed.

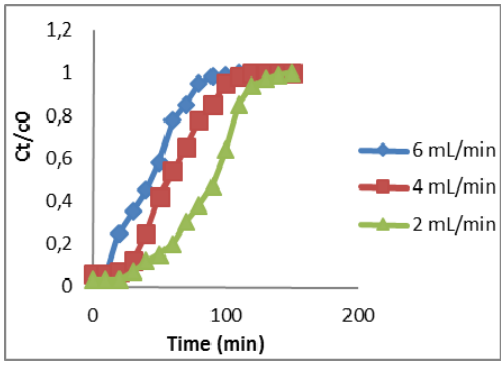

Fig. 4 Breakthrough curves of the effect of flow rate on AO7 adsorption onto TES column

D. Effect of Activated Carbon Bed Height

The fixed bed study was carried out at different bed height of 5, 10 and 15 cm (3.5, 7 and 10.5 g) with influent AO7 concentration of 30 mg/L, 4 mL/min flow rate, and pH 7.04 and at 301 K.

Fig. 5 shows that the breakthrough time decreased with increasing the bed height and increasing by the way the number of sorption sites and the residence time of the AO7 in the column, thus increasing the removal efficiency of AO7 in the fixed bed system.

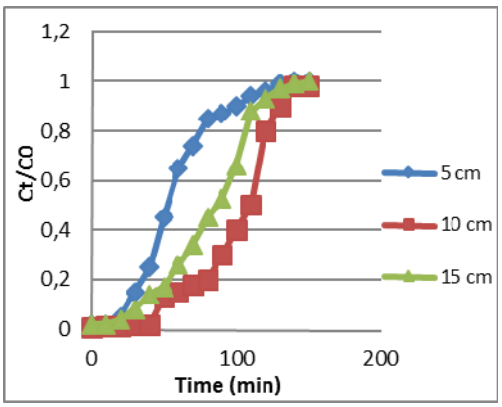

Fig. 5 Breakthrough curves for AO7 adsorption by TES at different bed heights

Fig. 5 shows the breakthrough curve obtained for AO7 adsorption on the TES. From Fig. 5, both the breakthrough and time increased with increasing the bed height. When the bed height increases, AO7 had more time to be in contact with TES that results in higher removal efficiency of AO7 in the column. So, the higher bed column results in a decrease in the solute concentration in the effluent at the same time. The slope of breakthrough curve decreased with increasing bed height, which resulted in a broadened mass transfer zone. A high adsorption capacity was observed at the highest bed height due to an increase in the surface area of adsorbent, which provided more binding sites for the adsorption.

The effect of bed height for adsorption of AO7 dye onto TES bed at heights of 5, 10 and 15 cm at influent concentration 30 ppm and flow rate 4 mL/min is shown in Fig. 5. This indicates that breakthrough time and the exhausting

time were increased from 30 to 120 and 10 to 105 min, respectively, when the bed height passed from 5 to 15 cm. The throughput volume of dye solution was increased with the increase in bed height due to the increase in surface area of adsorbent providing by the way, more binding sites for the adsorption and more number of sorption sites in general.

E. Dynamic Adsorption Models

1. Thomas Model

$$Ln\left[\frac{C_0}{C_t}-1\right]=\left[(k_{Th}q_0x/Q)-k_{Th}C_0t\right]$$

A linear plot of $Ln[(C_0/C_t)-1]$ against time (t) was employed to determine the Thomas parameters, that is, rate constant (k_{Th}), adsorption capacity (Qe), and correlation coefficient values (R^2) in which various experimental conditions for column adsorption of AO7 onto TES was conducted. The determined coefficients and relative constants were obtained using linear regression analysis and the results are listed in Table II.

TABLE II
THOMAS PARAMETERS FOR COLUMN ADSORPTION OF AO7 ONTO TES

initial concentration (mg/l)	flow rate (ml/min)	bed height (cm)	weight (g)	k_{Th} (ml/min.mg)	q_e (mg/g)	R^2
5	4	10	7	5,2	0,567	0,973
30	4	10	7	0,867	4,337	0,986
50	4	10	7	0,3	10,583	0,948
80	6	10	7	0,538	11,150	0,913
30	2	10	7	1,133	1,067	0,996
30	4	10	7	0,633	2,738	0,974
30	6	10	7	0,8	3,786	0,972
30	2	5	3,5	1,2	2,934	0,996
30	4	10	7	1,1	3,048	0,964
30	6	15	10,5	0,84	3,924	0,972

It indicates that rate constant increases with decreasing flow meter, initial concentration, and decreasing bed height. This is due to the driving force of adsorption process that is the difference between the concentration of AO7 in the solution and on the adsorbent. In addition, the value of equilibrium adsorption capacity (q_0) increases with the increase in bed height and initial concentration and also, with the increase of flow rate. So, contradictory effects have been found using higher flow rate and initial concentration for adsorption of AO7 on TES column. The maximum adsorption capacity related to Thomas model was found to be 11,15 mg/g at flow rate of 6 mL/min controlling initial concentration of 80 ppm, pH 7.04, and bed height of 10 cm. Also, all the results were well fitted to Thomas model with high values of correction coefficients R^2 of THOMAS model ranged from 0.913 to 0.996, indicating good linearity and indicating that Thomas model is suitable for sorption of AO7 with TES.

2. The Adams and Bohart Model

$$Ln\left(\frac{C_t}{C_0}\right)=k_{AB}C_0t-k_{AB}N_0Z/F$$

A linear plot of $Ln(C_t/C_0)$ against time (t) was obtained; values of k_{AB} and N_0 from the intercept and slope of the plot. The Adam's–Bohart adsorption model was applied to experimental data for the description of the initial part of the breakthrough curve. For all breakthrough curves, respective values of N_0, and k_{AB} were calculated and presented in Table III together with the correlation coefficients ($R^2 > 0.73$).

TABLE III
ADAMS AND BOHART PARAMETERS FOR COLUMN ADSORPTION OF AO7 ONTO TES

initial concentration (mg/l)	flow rate (ml/ min)	bed height (cm)	weight (g)	k_{AB} (ml/min. mg)	N_0 (mg/g)	R^2
5	4	10	7	6,6	0,522	0,972
30	4	10	7	0,833	3,625	0,986
50	4	10	7	0,38	6,620	0,979
80	4	10	7	0,275	8,899	0,967
30	2	10	7	0,9	0,915	0,938
30	4	10	7	0,967	1,743	0,917
30	6	10	7	0,567	3,508	0,903
30	4	5	3,5	1,167	4,269	0,934
30	4	10	7	0,9	2,554	0,908
30	4	15	10,5	1,333	1,228	0,835

Table II demonstrates Adams and Bohart parameters (k_{AB} and N_0) and its correlation coefficient value at different experimental conditions. It indicates that value k_{AB} increases with decreasing flow rate and decreasing initial concentration, increasing bed height. Also, values of N_0 were increased with increasing initial concentration and flow rate and decreasing bed height. The maximum adsorption capacity calculated based on Adams and Bohart model was found to be 8,89 mg/g at initial concentration of 80 ppm. in the case of Bohart–Adams model, low correlation coefficient (R^2 (<0.90) is observed, which indicate that Bohart–Adams model is not as appropriate a predictor for the breakthrough curve.

3. The Yoon–Nelson Model

$$Ln\left(\frac{C_t}{C_0-C_t}\right)=k_{YN}t-\tau k_{YN}$$

Yoon–Nelson model was applied to the experimental data with respect to flow rate, influent concentration of AO7, bed depth, and pH. A linear regression analysis was used on each set of data. A linear plot of $Ln[C_t/(C_0-C_t)]$ against sampling time (t) to determine the Yoon–Nelson model parameters of k_{YN} (rate constant), τ (50% breakthrough time), and k_{0YN} (adsorption capacity) are depicted in Table IV. The correlation coefficient values of each experiment are mentioned in Table IV.

It is clear that as the flow rate increases, the value of k_{0YN} and τ increase, but k_{YN} decreases and when initial concentration increases, the value of k_{0YN} and τ increase, but k_{YN} decreases.

As the bed height increases, the value of k_{YN} and τ increase, but k_{0YN} decreases. Regression coefficient values (< 0.90) indicate that data do not fit well Yoon–Nelson model.

TABLE IV
YOON NELSON PARAMETERS FOR COLUMN ADSORPTION OF AO7 ONTO TES

initial concentration (mg/l)	flow rate (ml/min)	bed height (cm)	weight (g)	k_{YN} (l/min)	τ (min)	R^2	q_{0YN} (mg/g)
5	4	10	7	0,03	195,97	0,978	0,560
30	4	10	7	0,024	271,71	0,978	4,658
50	4	10	7	0,016	353,69	0,968	10,105
80	4	10	7	0,016	374,31	0,963	17,111
30	2	10	7	0,034	127,12	0,974	1,090
30	4	10	7	0,032	132,42	0,929	2,270
30	6	10	7	0,031	130,42	0,861	3,354
30	4	5	3,5	0,036	174,17	0,943	5,971
30	4	10	7	0,028	205,71	0,914	3,527
30	4	15	10,5	0,038	161,82	0,851	1,850

V. CONCLUSION

The fixed-bed column adsorption of AO7 dye onto TES was investigated in the present study. The breakthrough curve (C_t/C_0 vs time) for various parameters of flow rate, initial AO7 concentration, bed height, and pH was plotted. The breakthrough time and exhaust time were increased with increasing flow rate, and bed height and decreasing initial AO7 concentration. The experimental data were applied to Thomas, Yoon–Nelson and Adams and Bohart model. The maximum adsorption capacity related to Thomas model was found to be 11.15 mg/g at initial concentration of 80 ppm at constant flow rate of 6 mL/min, bed height of 10 cm, and pH 7,04 with R^2 = 0.913. The Thomas model was found more fitted than other models, that is, Yoon–Nelson, and Adams and Bohart models derived from correlation coefficient.

REFERENCES

[1] J.F. Osma, V. Saravia, J.L. Toca-Herrera, S.R. Couto, Sunflower seed shells: a novel and effective low-cost adsorbent for the removal of the diazo dye Reactive Black 5 from aqueous solutions, J. Hazard. Mater. 147 (2007) 900–905.
[2] G.M.B. Soares, M.T.P. Amorim, R. Hrdina, M. Costa-Ferreira, Studies on the biotransformation of novel diazo dyes by laccas, Process Biochem. 37 (2002) 581–587.
[3] X.Y. Yang, B. Al-Duri, Application of branched pore diffusion model in the adsorption of reactive dyes on activated carbon, Chem. Eng. J. 83 (2001) 15–23.
[4] O.T. Mahony, E. Guibal, J.M. Tobin, Reactive dye biosorption by Rhizopus arrhizus biomass, Enzyme Microb. Technol. 31 (2002) 456–463.
[5] E.K. Raymound, F. Dunald, Encyclopedia of Chemical Technology, Wiley, New York, 1984.
[6] S. Papic, N. Koprivanac, A.L. Bozic, A. Metes, Removal of some reactive dyes from synthetic wastewater by combined Al(III) coagulation/carbon adsorption process, Dyes Pigments 62 (2004), 291–208.
[7] J.M. Chern, S.N. Huang, Study of nonlinear wave propagation theory. 1. Dye adsorption by activated carbon, Ind. Eng. Chem. Res. 37 (1998) 253–257.
[8] M. Ozacar, I.A. Sengil, Adsorption of reactive dyes on calcined alunite from aqueous solutions, J. Hazard. Mater. B 98 (2003) 211–224.
[9] J.M. Chern, Y.W. Chien, Adsorption of nitrophenol onto activated carbon: isotherms and breakthrough curves, Water Res. 36 (2002) 647–655.
[10] S. Singh, V.C. Srivastava, I.D. Mall, Fixed-bed study for adsorptive removal of furfural by activated carbon, Colloids Surf A: Physicochem. Eng. Aspects 332 (2009) 50–56.
[11] G. Vazquez, R. Alonso, S. Freire, J. Gonzalez-Alvarez, G. Antorrena, Uptake of phenol from aqueous solutions by adsorption in a Pinus pinaster bark packed bed, J. Hazard. Mater. B 133 (2006) 61–67.
[12] G.M.Walker, L.R. Weatherley, Adsorption of acid dyes onto granular activated carbon in fixed bed, Water Res. 31 (1997) 2093–2101.
[13] J.M. Chern, Y.W. Chien, Competitive adsorption of benzoic acid and pnitrophenol onto activated carbon: isotherm and breakthrough curves, Water Res. 37 (2003) 2347–2356.
[14] T.V.N. Padmesh, K. Vijayaraghavan, G. Sekaran, M. Velan, Biosorption of Acid Blue 15 using fresh water macroalga Azolla filiculoides: batch and column studies, Dyes Pigments 71 (2006) 77–82.
[15] C. Sourja, D. Sirshendu, D.G. Sunando, K.B. Jayanta, Adsorption study for the removal of a basic: experimental and modeling, Chemosphere 58 (2005) 1079–1086.
[16] M.J. Martin, A. Artola, M.D. Balaguer, M. Rigola, Activated carbons developed from surplus sewage sludge for the removal of dyes from dilute aqueous solutions, Chem. Eng. J. 94 (2003) 231–239.
[17] B.S. Girgis, A.A. El-Hendawy, Porosity development in activated carbons obtained from date pits under chemical activation with phosphoric acid, Micropor. Mesopor. Mater. 52 (2002) 105–117.
[18] Y. Diao, W.P. Walawender, L.T. Fan, Activated carbons prepared from phosphoric acid activation of grain sorghum, Bioresour. Technol. 81 (2002) 45–52.
[19] M. Jagtoyen, F.J. Derbyshire, Activated carbons from yellow poplar and white oak by H3PO4 activation, Carbon 36 (1998) 1085–1097.
[20] F. Suarez-Garcia, A. Martinez-Alonso, J.M.D. Tascon, Pyrolysis of apple pulp: chemical activation with phosphoric acid, J. Anal. Appl. Pyrol. 63 (2002) 283–301.
[21] T. Vernersson, P.R. Bonelli, E.G. Cerrella, A.L. Cukierman, Arundo donax cane as a precursor for activated carbons preparation by phosphoric acid activation, Bioresour. Technol. 83 (2002) 95–104.
[22] J. Guo, A.C. Lua, Textural and chemical properties of adsorbent prepared from palm shell by phosphoric acid activation, Mater. Chem. Phys. 80 (2003) 114–119.
[23] A. Kapoor, T. Viraraghavan, Removal of heavy metals from aqueous solutions using immobilized fungal biomass in continuous mode Water Research, 32, (1998) 1968–1977.
[24] M.S. Solum, R.J. Pugmire, M. Jagtoyen, F. Derbyshire, Evolution of carbon structure in chemically activated wood, Carbon 33 (1995) 1247–1254.
[25] Y.H. Yoon, J.H. Neslson, Application of gas adsorption kinetics, I. A theoretical model for respirator cartridge service life, Am. Ind. Hyg. Assoc. J., 45, (1984) 409–516.
[26] A. Wolborska, Adsorption on activated carbon of p-nitrophenol from aqueous solution, Water Research, Volume 23, Issue 1, January 1989, Pages 85–91.